Klein tunneling and electron optics in Dirac-Weyl fermion systems with tilted energy dispersion

V. Hung Nguyen* and J.-C. Charlier
Institute of Condensed Matter and Nanosciences, Université catholique de Louvain, Chemin des étoiles 8, B-1348 Louvain-la-Neuve, Belgium

(Received 14 November 2017; revised manuscript received 6 March 2018; published 11 June 2018)

The transport properties of relativisticlike fermions have been extensively studied in solid-state systems with isotropic energy dispersions. Recently, several two-dimensional and three-dimensional Dirac-Weyl (DW) materials exhibiting tilted energy dispersions around their DW cones have been explored. Here, we demonstrate that such a tilt character could induce drastically different transport phenomena, compared to the isotropic-dispersion cases. Indeed, the Klein tunneling of DW fermions of opposite chiralities is predicted to appear along two separated oblique directions. In addition, valley filtering and beam splitting effects are easily tailored by dopant engineering techniques whereas the refraction of electron waves at a (p-n)-doped interface is dramatically modified by the tilt, thus paving the way for emerging applications in electron optics and valleytronics.

DOI: 10.1103/PhysRevB.97.235113

I. INTRODUCTION

The observation of Dirac-like fermions in graphene [1] opened the door to explore the relativistic physics in condensed-matter systems [2]. Among many remarkable phenomena already discovered, the Klein tunneling [3] is direct evidence and concurrently provides a playground for implementing tests of relativistic quantum dynamics of these quasiparticles in a simple experimental situation [4]. In addition, these Dirac fermions with a linear energy dispersion exhibit several behaviors analogous to light rays in optical media [5], such as refraction, reflection, and Fabry-Pérot interferences, making the host material an ideal platform for electron optics and novel quantum device development [3,6–10].

In such scientific context, soon after the discovery of graphene, the search for materials hosting relativisticlike particles has hence become an emerging topic. Actually, the Dirac-Weyl (DW) fermions have been explored in several two-dimensional (2D) and three-dimensional (3D) materials. Silicene, germanene, stanene, graphynes, phosphorene, borophene allotropes [11–16], etc., correspond to the 2D form. Examples in the 3D form include Na_3Bi, Cd_3As_2, the monopnictide family (NbP, NbAs, TaP, and TaAs), the HgTe class, LaAlGe, $Mo_xW_{1-x}Te_2$, $SrSi_2$, Ta_3S_2, and 3D carbon networks [17–26]. Interestingly, the appearance of these DW materials resulted in the exploration of several novel phenomena [27], e.g., quantum oscillations [28], a chiral anomaly [29], chirality-dependent Hall effects [30,31], Klein tunneling, electron optics in 3D systems [32], photovoltaic effects [33], etc.

In contrast to graphene, the DW cones in several materials [13–18,20–25] are anisotropic and could be exceptionally tilted. Remarkably, the tilt character has been shown to affect strongly the electronic transport and the optical properties of these DW fermions [34–42]. For instance, the small (subcritical) tilts give rise to an asymmetric Pauli blockade, resulting in finite free-electron Hall response [39] and nonzero photocurrents [41]. For large (overcritical) tilts as in type-II Weyl semimetals [27], the Fermi surface is no longer pointlike, inducing other novel phenomena. For example, the Landau-level spectrum is gapped and has no chiral zero mode if the direction of the magnetic field is outside the Weyl cone [35]. The anomalous Hall conductivity is not universal and can change sign as a function of the tilt magnitude [36]. It is worth noting that, even being an inherent property of materials, the DW dispersion (hence, the tilt character) can be also generated and tuned, e.g., either by strain or by nanoengineering techniques [13,14,16,21,24].

These observations give rise to questions about the effects of this tilt character on crucial phenomena, such as Klein tunneling and electron optics in the DW fermion systems. In this paper, we explore novel transport properties of DW fermions in heterodoped structures induced by the effects of subcritical tilt. In particular, we find that, instead of being observed in a unique direction (i.e., normal incidence) as in the nontilted case, the Klein tunneling of tilted DW fermions of opposite chiralities is achieved in two separated oblique directions. In addition, interesting phenomena, such as anisotropic Fabry-Pérot resonances, valley filtering and beam splitting effects, and other novel electron optics behaviors in DW p-n junctions are also predicted. Besides their importance to fully understand the relativisticlike phenomena of DW fermions, our findings could be the basis for novel applications in electron optics and valleytronics.

II. METHODS

Around the DW cones, charge carriers can be modeled by a generic Hamiltonian [36–41],

$$H_0 = \sum_{\iota=x,y,z} \tau_c(u_\iota p_\iota + \sigma_\iota v_{F\iota} p_\iota), \tag{1}$$

where σ_ι are Pauli's matrices, τ_c represents the chirality, and $\vec{u} = (u_x, u_y, u_z)$ describes the tilt of energy dispersion. Since they always appear in pairs with opposite chiralities, $\tau_c = \pm 1$

*viet-hung.nguyen@uclouvain.be

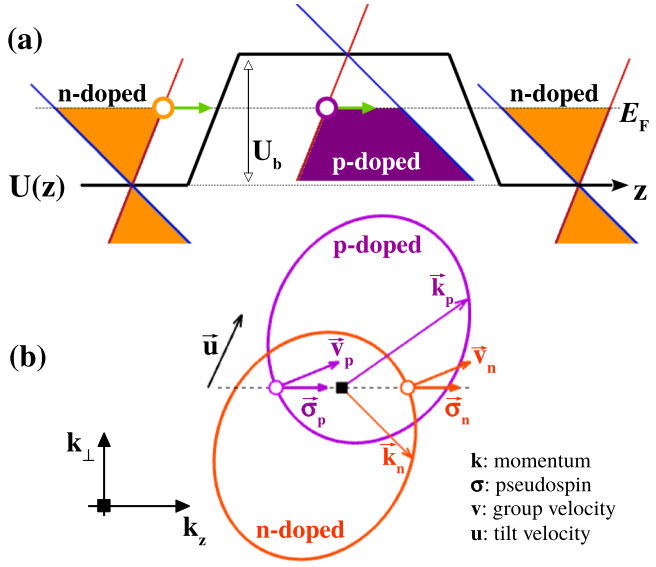

FIG. 1. Potential barrier in Dirac-Weyl fermion systems with a tilted energy dispersion. (a) Energy profile (barrier height: U_b) along the transport direction (i.e., Oz axis). (b) Diagram illustrating the momentum shift of Fermi surfaces in the differently doped zones and the transmission process with momentum $\vec{k}_\perp = 0$. The subscripts n/p indicate the vectors outside/inside the barrier, respectively, and the black-dashed line implies the $\vec{k}_\perp$ conservation.

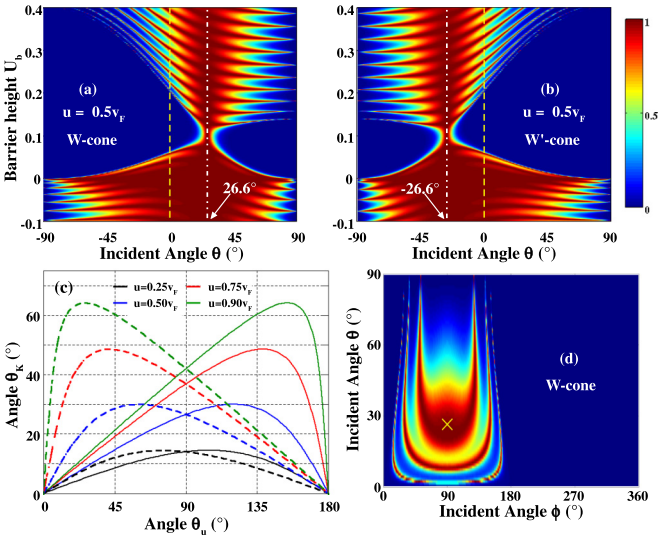

FIG. 2. Klein tunneling and Fabry-Pérot resonances. (a) and (b) (U_b,θ) maps of transmission probabilities ($\mathcal{T}_{W,W'}$) of tilted DW fermions in the W and W' cones, respectively. The incident energy $E = 0.1$, the incident angle $\phi = 90°$, and the barrier width $L_b = 200a_0$, whereas the $\vec{u}$ direction is $(\theta_u,\phi_u) = (90°,90°)$. (c) Klein tunneling direction θ_K obtained for the W (solid lines) and W' cones (dashed lines) as a function of θ_u. (d) represents a $(\phi$-$\theta)$ map of $\mathcal{T}_W$ at $U_b = 0.2$ in (a). The cross symbol marks the Klein tunneling direction.

for the W and W' cones. We consider heterodoped structures modeled by applying a potential profile $U(z)$ along the Oz axis (see Fig. 1), and accordingly the system Hamiltonian reads $H = H_0 + U(z)$. In order to compute the transport properties, we employ the calculation method developed in Ref. [43]. In particular, H is separated into two independent parts, i.e., $H = H_z + H_\perp$, and then is rewritten in the basis $\{|z_m\rangle \otimes |\vec{k}_\perp\rangle\}$ with the mesh-spacing $a_0 = z_{m+1} - z_m$ along the transport direction (i.e., Oz axis) and the plane-wave $|\vec{k}_\perp\rangle$ on the Oxy plane. This Hamiltonian is finally solved using the Green's-function technique, and the transport properties are extracted (see the Supplemental Material in Ref. [44] for more details).

The energy eigenvalues of the Hamiltonian (1) are given by $E_{\tau_c\tau_b}(\vec{k}) = \hbar(\tau_c\vec{u}\vec{k} + \tau_b|\vec{\xi}_{\vec{k}}|)$ where the vector $\vec{\xi}_{\vec{k}} = (v_{Fx}k_x, v_{Fy}k_y, v_{Fz}k_z)$ and $\tau_b = \pm 1$ correspond to the conduction/valence bands, respectively. Accordingly, the pseudospin and group velocity are determined as $\vec{\sigma}_{\tau_c\tau_b}(\vec{k}) = \tau_c\tau_b\vec{\xi}_{\vec{k}}$ and $\vec{v}_{\tau_c\tau_b}(\vec{k}) = \tau_c\vec{u} + \tau_b\vec{\eta}_{\vec{k}}/|\vec{\xi}_{\vec{k}}|$ with $\vec{\eta}_{\vec{k}} = (v_{Fx}^2k_x, v_{Fy}^2k_y, v_{Fz}^2k_z)$ (see the Supplemental Material [44]). Some exceptional features, compared to the isotropic dispersion case, are found here. First, the group-velocity $\vec{v}$ and momentum $\vec{k}$ are no longer collinear. Note that the direction of $\vec{v}$ (but not of $\vec{k}$) determines the propagating direction of an electron wave in the crystal. Second, the pseudospin is no longer locked to the direction of electron motion. Third, the center of the Fermi surface in momentum space is energy dependent due to the tilt, offering the possibility to separate and to control this separation of Fermi surfaces in heterodoped systems as illustrated in Fig. 1(b). These features lay the foundations to observe the novel transport phenomena reported in this article.

Unless otherwise stated, to concentrate on the tilting effects, the velocities v_{Fi} in Eq. (1) are assumed to be isotropic, i.e., $v_{Fx} \equiv v_{Fy} \equiv v_{Fz} = v_F$. Throughout the paper, three vectors $\vec{v}$, $\vec{u}$, and $\vec{\sigma}$ are considered in the same form [i.e., $\vec{v} = v(\sin\theta\cos\phi, \sin\theta\sin\phi, \cos\theta)$, etc.], and the energies are presented in the unit of $E_0 = \hbar v_F/2a_0$.

III. RESULTS

A. Klein tunneling and Fabry-Pérot interferences

Transmission probabilities $\mathcal{T}_{W,W'}$ of tilted DW fermions through a potential barrier [see Fig. 1(a)] are displayed in Figs. 2(a) and 2(b), respectively, as a function of barrier height U_b and incident angle θ. Without the tilt [3,5,32], the transmission exhibits two well-known phenomena: $\mathcal{T}_{W,W'} = 1$ at $\theta = 0°$, independent of U_b (i.e., Klein tunneling), and resonant peaks in oblique directions (i.e., Fabry-Pérot interferences). Under the tilting effects, a novel feature is observed: The Klein tunneling is still preserved but is achieved in two separated oblique directions θ_K for the DW fermions of opposite chiralities. In particular, these Klein tunneling directions are determined by group-velocities $\vec{v}_K = v_F\vec{e}_z + \tau_c\vec{u}$ with the unit vector $\vec{e}_z$ along the Oz axis, e.g., $\theta_K = \tau_c\cos^{-1}[(v_F + \tau_c u_z)/\sqrt{(v_F + \tau_c u_z)^2 + u_\perp^2}] \simeq \pm 26.6°$ for $u = 0.5v_F$ considered in Figs. 2(a) and 2(b). Note that if the $\vec{u} \parallel Oz$ axis (i.e., $u_\perp = 0$), all transport phenomena induced by the tilting effects disappear, i.e., the similar pictures as in the nontilted case [32] are observed.

To clarify these results, the transmission probability $\mathcal{T}$ was computed analytically in the ideal case of abrupt barriers using matching of the wave functions at the barrier interfaces (see the details in the Supplemental Material [44]). In such a case,

its momentum dependence is given by

$$\mathcal{T} = |f(\vec{k}_n,\vec{k}_p,0)/f(\vec{k}_n,\vec{k}_p,L_b)|^2, \quad (2)$$

where $f(\vec{k}_n,\vec{k}_p,L_b) = \sin\frac{\theta^+_{\sigma n}-\theta^-_{\sigma p}}{2}\sin\frac{\theta^-_{\sigma n}-\theta^+_{\sigma p}}{2}e^{-ik^+_{pz}L_b} - \sin\frac{\theta^+_{\sigma n}-\theta^+_{\sigma p}}{2}\sin\frac{\theta^-_{\sigma n}-\theta^-_{\sigma p}}{2}e^{-ik^-_{pz}L_b}$. Here, the subscripts n/p indicate the quantities in n-doped/p-doped zones [see Fig. 1(a)], angles $\theta^\pm_\sigma$ (vectors $\vec{k}^\pm$) determine the directions of pseudospin (momenta) in the transmitted and reflected states, respectively, and L_b is the barrier width. It has been well known that the Klein tunneling is observed, satisfying the pseudospin conservation [3]. With $\vec{\sigma}_{\tau_c\tau_b} = \tau_c\tau_b\vec{k}/k$ and the conservation of $\vec{k}_\perp$, the conservation $\vec{\sigma}^+_n \equiv \vec{\sigma}^+_p$ is actually obtained only for $\vec{k}_\perp = 0$ [see Fig. 1(b)], and hence the second term of $f(\vec{k}_n,\vec{k}_p,L_b)$ vanishes ($\theta^+_{\sigma n} = \theta^+_{\sigma p}$). Accordingly, the transmission $\mathcal{T} = 1$ is achieved, independent of U_b and L_b, which demonstrates the Klein tunneling effect. The corresponding group-velocity $\vec{v}_K = v_F\vec{e}_z + \tau_c\vec{u}$ is exactly the one reported above. Note that the same velocity $\vec{v}_K$ is achieved in differently doped zones, i.e., the Klein tunneling is a refractionless transmission. Thus, the origin of the deflected Klein tunneling is simply the noncollinearity of $\vec{v}$ and $\vec{k}$ induced by the tilting effects.

In Fig. 2(c), the dependence of the Klein tunneling direction (i.e., direction of $\vec{v}_K$) on the tilt velocity $\vec{u}$ is presented. Whereas θ_K is a function of both u and θ_u, angle ϕ_K is simply determined by $\phi_K = \phi_u + (1-\tau_c)90^\circ$. Note that the direction $(\theta_K,\phi_K + 180^\circ)$ for $\tau_c = -1$ is actually equivalent to $(-\theta_K,\phi_K)$ in Fig. 2(b). As presented in Fig. 2(c), a large deflection of the Klein tunneling is predicted when increasing the tilt velocity, i.e., θ_K can reach maximum values of $\sim 30^\circ$ and $\sim 50^\circ$ for $u = 0.5v_F$ and $0.75v_F$, respectively. Interestingly, except for the $\vec{u} \parallel Oz$ axis, the significant effects can be obtained in a wide range of θ_u, especially when the tilt magnitude is large.

In addition, Figs. 2(a) and 2(b) demonstrate that the Fabry-Pérot resonant spectra can be also significantly deflected when the energy dispersion is tilted. This deflection is more clearly observed in Fig. 2(d) where the transmission probability for the W cone is illustrated as a function of incident angles θ and ϕ. Indeed, instead of being isotropic with respect to angle ϕ [32] for a nontilted dispersion, the resonant spectra become strongly anisotropic under the tilting effects, i.e., depending on both angles θ and ϕ. Besides its dependence on the noncollinearity of $\vec{v}$ and $\vec{k}$, the deflection of Fabry-Pérot resonances can be basically explained as a consequence of the momentum shift of the Fermi surfaces as illustrated in Fig. 1(b). Indeed, this shift, together with the conservation of $\vec{k}_\perp$, allows for finite transmission only in certain directions. The similar picture is achieved for the W' cone, except that the resonant peaks occur in opposite directions.

Note additionally that, since the noncollinearity of $\vec{v}$ and $\vec{k}$ is one of the key elements, the deflection of highly transparent directions (i.e., Klein tunneling and Fabry-Pérot resonances) can also be obtained thanks to the anisotropic character of energy dispersion (see the demonstration in the Supplemental Material [44]), i.e., when $v_{Fx,Fy,Fz}$ are not identical. Different from the tilting effects, this anisotropy however does not include a momentum shift of the Fermi surfaces and results in the same deflection for fermions of opposite chiralities. In general, the deflection of transparent directions reported here can be induced by the combined effects of these two characters of DW fermions. At last, it is worth noting that, in addition to the pseudospin conservation, the Klein tunneling in all cases is found to exhibit another inherent property: refractionless character, i.e., the same velocity $\vec{v}_K$ is achieved in differently doped zones as mentioned above.

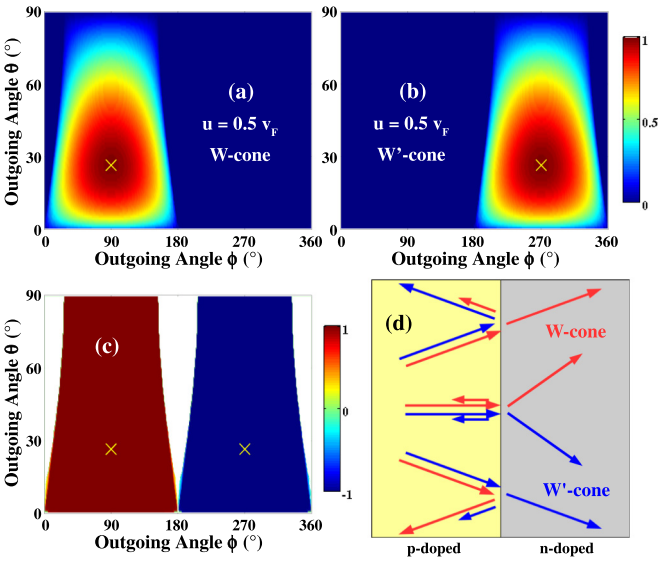

FIG. 3. Valley filtering and beam splitting. (a) and (b) (ϕ-θ) maps of transmission probabilities $\mathcal{T}_{W,W'}$ in a p-n junction and (c) the corresponding valley polarization. The the blank regions in (c) correspond to the fully reflective directions. The barrier height is $U_b = 0.2$ whereas the other parameters are the same as in Fig. 2. The cross symbols mark the Klein tunneling directions. (d) Schematics of directional separation and beam splitting effects of valley-dependent currents.

B. Valleytronics and electron optics in *p-n* junctions

In analogy with the valley indices in graphene [45], the two chiralities of DW fermions could be used as new degrees of freedom to store and carry information in valleytronic devices [30,41]. The separated Klein tunneling directions of opposite chiralities observed in Fig. 2 suggest that valley (i.e., chirality) filtering and beam splitting effects can be obtained here. Simultaneously, the electron optics behaviors [32] in DW p-n junctions can be drastically modified by the tilting effects.

In Fig. 3, the transmission probabilities $\mathcal{T}_{W,W'}$ through a p-n junction and the corresponding valley polarization $P_{val} = (\mathcal{T}_W - \mathcal{T}_{W'})/(\mathcal{T}_W + \mathcal{T}_{W'})$ are computed and presented as a function of outgoing angles θ and ϕ. First, due to the momentum shift of the Fermi surfaces, the transmission of each DW cone is allowed only in certain directions (as already mentioned), and these transparent directions for two cones can be totally separated if the tilt is sufficiently large [see Figs. 3(a) and 3(b)]. Consequently, strong valley filtering with perfect valley polarization can be obtained as depicted in Fig. 3(c) and schematically described in Fig. 3(d). Moreover, due to the deflected Klein tunneling, the transmission probability exhibits peaks at two separated directions for the two cones [see the marked points in Figs. 3(a)–3(c)]. Hence, the high

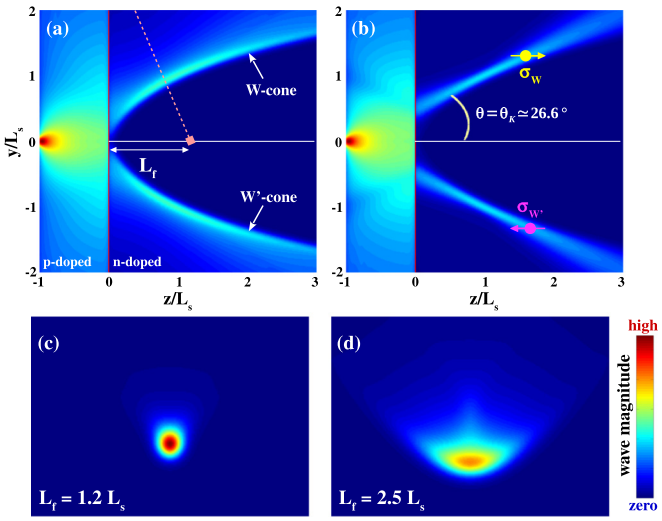

FIG. 4. Electron wave propagation in ***p-n*** junctions with (a) short and (b) long gradient widths of the doping profile: $L_b = 100a_0$ and $900a_0$, respectively. Electron waves are injected from a source point at $(0,0,-L_s)$ with a distance L_s ($L_s \gg L_b$) from the p-n interface. (c) and (d) represent the cut planes in (a), which are parallel to the Ox axis and perpendicular to the Klein tunneling direction of the W cone [see the dashed line in (a)] with two different distances L_f. Here, $E = 0.1$, $U_b = 0.2$, and $\vec{u} = u(0,1,0)$ with $u = 0.5v_F$.

valley-dependent currents are always obtained around these two directions independently on the barrier height and carrier energy. In addition, the high reflection directions of fermions with opposite chiralities are also separated, implying that both the transmitted and the reflected beams can be highly valley polarized as schematically described in Fig. 3(d).

The beam slitting effect (see also Fig. 4) is most obviously demonstrated when considering the normal incident beam, i.e., $\vec{v}_\perp = 0$ (or $\vec{k}_\perp = \tau_c k_p \vec{u}_\perp / v_F$) in the p-doped zone. In such a case, $\vec{v}_\perp = \tau_c(1 + k_p/k_n)\vec{u}_\perp$ in the n-doped zone is obtained. Indeed, the outgoing beam is split with opposite group-velocities $\vec{v}_\perp$ for fermions of opposite chiralities [see the diagrammatic description in Fig. 3(d)]. Interestingly, this effect depends not only on $\vec{u}_\perp$, but also on the ratio k_p/k_n, which is tunable by controlling the doping profile.

At last, the tilting effects on the optical-like behaviors of DW fermions in p-n junctions should be clarified. The refraction of electron waves at the p-n interface in the isotropic dispersion case is known to satisfy Snell's law with negative refractive indices, inducing the Veselago focusing effect [5–8,32]. This picture can be dramatically disturbed by the tilting effects (see Fig. 4). To mimic the electron optics behaviors, the propagation of electron waves presented in Fig. 4 was computed using a semiclassical billiard model (see the Supplemental Material in Ref. [44] for more details). Actually, starting from Snell's law, the tilting effects are found to split the outgoing waves of opposite chiralities into opposite directions [see Figs. 4(a) and 4(b)], thus inducing both the positive (around the Klein tunneling directions) and the negative refraction indices [44]. As an amazing result, the tilted DW system exhibits two focusing points for opposite chiralities as displayed in Figs. 4(a), 4(c), and 4(d) whereas a unique point is observed in the normal direction of the isotropic fermion systems [6,32,44].

In addition, although all the other transmissions can be strongly affected, the Klein tunneling is a unique one that is insensitive to an increase in gradient width between highly doped zones [5]. This property has been demonstrated to be a potential for designing Klein collimators [46] when the gradient width is long enough. In such a case, the tilted DW systems represent two separated oblique collimation directions for opposite chiralities as clearly visible in Fig. 4(b). Moreover, besides owning two opposite chiralities, these two Klein collimated beams also possess well-defined and antiparallel pseudospins, i.e., $\vec{\sigma}_{\tau_c} = \tau_c \vec{\xi}_K$, thus offering promising possibilities in both valleytronics and pseudospintronics.

IV. DISCUSSION AND CONCLUSION

First, the DW cones in DW semimetals are not always energy isolated from the trivial bands, and hence, for some specific materials, the contribution of these trivial bands should be estimated to compute the total current through the system. In this regard, we would like to emphasize that using the simple Hamiltonian (1), the main aim of the current paper, is to clarify the novel transport phenomena of tilted DW fermions, compared to the case of isotropic ones. Additionally, it has been shown that, in general, the DW fermions with linear energy dispersion exhibit extremely high Fermi velocity and carrier mobility [47], compared to the normal electrons. In order to observe the electron-optic behaviors (e.g., Veselago lens and Klein collimation) of DW fermions, the system size is always required to be much larger, i.e., typically about hundreds of nanometers to micrometers [8–10], than its de Broglie wavelength. In such a large-scale system, the DW fermions with high mobility can represent a major contribution to the measured current whereas the normal charge carriers (in the cases mentioned above) should be strongly affected by scatterings.

Second, experimental confirmation of the phenomena explored in this paper requires the realization and controllability of the system doping profile. In this regard, the electrostatic doping could be considered as the most appropriate technique. Note that our findings are valid in both 2D and 3D DW systems. Although it has been demonstrated in 2D cases, the electrostatic doping in 3D systems may require some further developments, in particular, to solve the issue of gate efficiency. In the latter case, some directions have already been demonstrated, i.e., the gate doping can be efficiently applied in DW thin films [48] and nanowires [49]. However, another issue, i.e., finite-size-induced confinements, could arise and should be taken into account. In particular, a crossover from 3D to 2D electronic behaviors was observed in Ref. [50] when the thickness is reduced below 26 nm whereas the characteristic of Dirac particles was still observed in Ref. [51] with a film thickness of 18 nm. In addition, the directionally separated currents predicted can be measured using multiple directional leads as in Refs. [8,9].

To conclude, with tilted energy dispersions, DW fermions possess some exceptional properties: (i) noncollinearity of $\vec{v}$ and $\vec{k}$ (similarly, $\vec{v}$ and pseudospin $\vec{\sigma}$) and (ii) momentum shift of the Fermi surface when varying the carrier energy. These properties dramatically modify their transport properties when compared to the isotropic dispersion case. In particular, the Klein tunneling of tilted fermions of opposite chiralities

is observed in two separated oblique directions instead of occurring in a unique one (i.e., normal incidence) as in the nontilted case. In addition, all electron-optic behaviors in the heterodoped junctions can be strongly modified by the tilt thus inducing possible valley filtering and beam splitting effects. To summarize, the present paper highlights the outstanding transport properties of tilted DW fermions that could pave the way for novel applications of the host materials in electron optics and valleytronics.

ACKNOWLEDGMENTS

V.H.N. and J.-C.C. acknowledge financial support from the F.R.S.-FNRS of Belgium through the research Project (Project No. T.1077.15), from the Fédération Wallonie-Bruxelles through the ARC on 3D architecturing of 2D crystals (Grant No. 16/21-077), and from the European Union's Horizon 2020 Research and Innovation Program (Program No. 696656).

[1] K. S. Novoselov, A. K. Geim, S. V. Morozov, D. Jiang, M. I. Katsnelson, I. V. Grigorieva, S. V. Dubonos, and A. A. Firsov, Nature (London) **438**, 197 (2005).
[2] A. H. Castro Neto, F. Guinea, N. M. R. Peres, K. S. Novoselov, and A. K. Geim, Rev. Mod. Phys. **81**, 109 (2009).
[3] M. I. Katsnelson, K. S. Novoselov, and A. K. Geim, Nat. Phys. **2**, 620 (2006); A. F. Young and P. Kim, *ibid.* **5**, 222 (2009).
[4] P. Kim, in *Dirac Matter, Progress in Mathematical Physics* (Birkhäuser, Cham, 2017), Vol. 71, pp. 1–23.
[5] P. E. Allain and J. N. Fuchs, Eur. Phys. J. B **83**, 301 (2011).
[6] V. V. Cheianov, V. Fal'ko, and B. L. Altshuler, Science **315**, 1252 (2007).
[7] Q. Wilmart, S. Berrada, D. Torrin, V. Hung Nguyen, G. Fève, J.-M. Berroir, P. Dollfus, and B. Plaçais, 2D Mater. **1**, 011006 (2014); S. Morikawa, Q. Wilmart, S. Masubuchi, K. Watanabe, T. Taniguchi, B. Plaçais, and T. Machida, Semicond. Sci. Technol. **32**, 045010 (2017).
[8] G.-H. Lee, G.-H. Park, and H.-J. Lee, Nat. Phys. **11**, 925 (2015).
[9] S. Chen *et al.*, Science **353**, 1522 (2016).
[10] P. Bøggild, J. M. Caridad, C. Stampfer, G. Calogero, N. R. Papior, and M. Brandbyge, Nat. Commun. **8**, 15783 (2017).
[11] S. Balendhran, S. Walia, H. Nili, S. Sriram, and M. Bhaskaran, Small **11**, 640 (2015).
[12] D. Malko, C. Neiss, F. Viñes, and A. Görling, Phys. Rev. Lett. **108**, 086804 (2012).
[13] J. Kim *et al.*, Science **349**, 723 (2015); Y. Li and X. Chen, 2D Mater. **1**, 031002 (2014).
[14] Y. Lu *et al.*, NPJ Comput. Mater. **2**, 16011 (2016); C.-H. Li, Y.-J. Long, L.-X. Zhao, L. Shan, Z.-A. Ren, J.-Z. Zhao, H.-M. Weng, X. Dai, Z. Fang, C. Ren, and G.-F. Chen, Phys. Rev. B **95**, 125417 (2017).
[15] X.-F. Zhou, X. Dong, A. R. Oganov, Q. Zhu, Y. Tian, and H.-T. Wang, Phys. Rev. Lett. **112**, 085502 (2014); F. Ma, Y. Jiao, G. Gao, Y. Gu, A. Bilic, Z. Chen, and A. Du, Nano Lett. **16**, 3022 (2016); M. Nakhaee, S. A. Ketabi, and F. M. Peeters, Phys. Rev. B **97**, 125424 (2018).
[16] M. O. Goerbig, J.-N. Fuchs, G. Montambaux, and F. Piéchon, Phys. Rev. B **78**, 045415 (2008); H.-Y. Lu, A. S. Cuamba, S.-Y. Lin, L. Hao, R. Wang, H. Li, Y. Y. Zhao, and C. S. Ting, *ibid.* **94**, 195423 (2016).
[17] Z. Wang, Y. Sun, X.-Q. Chen, C. Franchini, G. Xu, H. Weng, X. Dai, and Z. Fang, Phys. Rev. B **85**, 195320 (2012); Z. K. Liu *et al.*, Science **343**, 864 (2014).
[18] Z. K. Liu *et al.*, Nat. Mater. **13**, 677 (2014); A. M. Conte, O. Pulci, and F. Bechstedt, Sci. Rep. **7**, 45500 (2017).
[19] Y. Xu, F. Zhang, and C. Zhang, Phys. Rev. Lett. **115**, 265304 (2015).
[20] H. Weng, C. Fang, Z. Fang, B. A. Bernevig, and X. Dai, Phys. Rev. X **5**, 011029 (2015); S.-Y. Xu *et al.*, Nat. Phys. **11**, 748 (2015); L. X. Yang *et al.*, *ibid.* **11**, 728 (2015).
[21] J. Ruan, S.-K. Jian, H. Yao, H. Zhang, S.-C. Zhang, and D. Xing, Nat. Commun. **7**, 11136 (2016).
[22] S.-Y. Xu *et al.*, Sci. Adv. **3**, e1603266 (2017).
[23] Y. Sun, S.-C. Wu, M. N. Ali, C. Felser, and B. Yan, Phys. Rev. B **92**, 161107(R) (2015); Y. Wu, D. Mou, N. H. Jo, K. Sun, L. Huang, S. L. Bud'ko, P. C. Canfield, and A. Kaminski, *ibid.* **94**, 121113(R) (2016).
[24] T.-R. Chang *et al.*, Nat. Commun. **7**, 10639 (2016).
[25] S.-M. Huang *et al.*, Proc. Natl. Acad. Sci. USA **113**, 1180 (2016); G. Chang *et al.*, Sci. Adv. **2**, e1600295 (2016).
[26] H. Weng, Y. Liang, Q. Xu, R. Yu, Z. Fang, X. Dai, and Y. Kawazoe, Phys. Rev. B **92**, 045108 (2015); A. Lherbier, H. Terrones, and J.-C. Charlier, *ibid.* **90**, 125434 (2014).
[27] N. P. Armitage, E. J. Mele, and A. Vishwanath, Rev. Mod. Phys. **90**, 015001 (2018).
[28] L. P. He, X. C. Hong, J. K. Dong, J. Pan, Z. Zhang, J. Zhang, and S. Y. Li, Phys. Rev. Lett. **113**, 246402 (2014).
[29] C.-L. Zhang *et al.*, Nat. Commun. **7**, 10735 (2016).
[30] S. A. Yang, H. Pan, and F. Zhang, Phys. Rev. Lett. **115**, 156603 (2015).
[31] A. A. Burkov, Phys. Rev. Lett. **113**, 187202 (2014).
[32] R. D. Y. Hills, A. Kusmartseva, and F. V. Kusmartsev, Phys. Rev. B **95**, 214103 (2017).
[33] K. Taguchi, T. Imaeda, M. Sato, and Y. Tanaka, Phys. Rev. B **93**, 201202(R) (2016).
[34] M. Trescher, B. Sbierski, P. W. Brouwer, and E. J. Bergholtz, Phys. Rev. B **91**, 115135 (2015); **95**, 045139 (2017).
[35] A. A. Soluyanov, D. Gresch, Z. Wang, Q. Wu, M. Troyer, X. Dai, and B. A. Bernevig, Nature (London) **527**, 495 (2015).
[36] A. A. Zyuzin and R. P. Tiwari, JETP Lett. **103**, 717 (2016).
[37] C. Yesilyurt, Z. B. Siu, S. G. Tan, G. Liang, and M. B. A. Jalil, J. Appl. Phys. **121**, 244303 (2017).
[38] G. Sharma, P. Goswami, and S. Tewari, Phys. Rev. B **96**, 045112 (2017).
[39] J. F. Steiner, A. V. Andreev, and D. A. Pesin, Phys. Rev. Lett. **119**, 036601 (2017).
[40] S. P. Mukherjee and J. P. Carbotte, Phys. Rev. B **96**, 085114 (2017).
[41] Q. Ma *et al.*, Nat. Phys. **13**, 842 (2017).
[42] C.-K. Chan, N. H. Lindner, G. Refael, and P. A. Lee, Phys. Rev. B **95**, 041104(R) (2017).
[43] V. Hung Nguyen, A. Bournel, P. Dollfus, J. Phys.: Condens. Matter **22**, 115304 (2010); K. M. Masum Habib, R. N. Sajjad, A. W. Ghosh, Appl. Phys. Lett. **108**, 113105 (2016).

[44] See Supplemental Material at http://link.aps.org/supplemental/10.1103/PhysRevB.97.235113, which includes Refs. [9,32,43,46,52,53]. In this material, the calculation methods, the analytical solution of transmission probability in Eq. (2), the refraction and reflection of electron waves at a *p*-*n* interface, and the effects of anisotropic energy dispersion are presented in detail.

[45] D. Xiao, W. Yao, and Q. Niu, Phys. Rev. Lett. **99**, 236809 (2007).

[46] F. Libisch, T. Hisch, R. Glattauer, L. A. Chizhova, and J. Burgdörfer, J. Phys.: Condens. Matter **29**, 114002 (2017); M.-H. Liu, C. Gorini, and K. Richter, Phys. Rev. Lett. **118**, 066801 (2017).

[47] C. Shekhar *et al.*, Nat. Phys. **11**, 645 (2015); T. Liang, Q. Gibson, M. N. Ali, M. Liu, R. J. Cava, and N. P. Ong, Nat. Mater. **14**, 280 (2015); A. Narayanan, M. D. Watson, S. F. Blake, N. Bruyant, L. Drigo, Y. L. Chen, D. Prabhakaran, B. Yan, C. Felser, T. Kong, P. C. Canfield, and A. I. Coldea, Phys. Rev. Lett. **114**, 117201 (2015); C.-L. Zhang, Z. Yuan, Q.-D. Jiang, B. Tong, C. Zhang, X. C. Xie, and S. Jia, Phys. Rev. B **95**, 085202 (2017); R. Sankar, G. Peramaiyan, I. P. Muthuselvam, C. J. Butler, K. Dimitri, M. Neupane, G. N. Rao, M.-T. Lin, and F. C. Chou, Sci. Rep. **7**, 40603 (2017).

[48] Y. Liu *et al.*, NPG Asia Mater. **7**, e221 (2015); L. Wang, I. Gutiérrez-Lezama, C. Barreteau, D.-K. Ki, E. Giannini, and A. F. Morpurgo, Phys. Rev. Lett. **117**, 176601 (2016); Y. Wang *et al.*, Nat. Commun. **7**, 13142 (2016); E. Zhang *et al.*, Nano Lett. **17**, 878 (2017).

[49] C.-Z. Li, L.-X. Wang, H. Liu, J. Wang, Z.-M. Liao, and D.-P. Yu, Nat. Commun. **6**, 10137 (2015); L.-X. Wang, C.-Z. Li, D.-P. Yu, and Z.-M. Liao, *ibid.* **7**, 10769 (2016); B.-C. Lin, S. Wang, L.-X. Wang, C.-Z. Li, J.-G. Li, D. Yu, and Z.-M. Liao, Phys. Rev. B **95**, 235436 (2017).

[50] F.-X. Xiang, A. Srinivasan, O. Klochan, S.-X. Dou, A. R. Hamilton, and X.-L. Wang, arXiv:1703.02741.

[51] J. Hellerstedt, I. Yudhistira, M. T. Edmonds, C. Liu, J. Collins, S. Adam, and M. S. Fuhrer, Phys. Rev. Mater. **1**, 054203 (2017).

[52] C. W. J. Beenakker, Phys. Rev. Lett. **97**, 067007 (2006).

[53] S. P. Milovanović, M. R. Masir, and F. M. Peeters, J. Appl. Phys. **115**, 043719 (2014); S. P. Milovanović, D. Moldovan, and F. M. Peeters, *ibid.* **118**, 154308 (2015).